Electronic Supplementary Material (ESI) for Journal of Materials Chemistry A.

Highly-efficient Photocatalytic Hydrogen Evolution Triggered by Spatial Confinement Effects over Co-crystal Templated Boron-doped Carbon Nitride Hollow Nanotubes

Wei Dai [a, b], Ranhao Wang [b], Zhijie Chen [b], Shimao Deng [b], Changzhu Huang [b], Wenjun Luo [a,*], Hong Chen [b,*]

[a] Faculty of Materials Science and Chemistry, China University of Geosciences, No. 68 Jincheng Street, Esat Lake High-tech Department Zone, Wuhan, Hubei, China.

[b] Shenzhen Key Laboratory of Interfacial Science and Engineering of Materials, State Environmental Protection Key Laboratory of Integrated Surface Water-Groundwater Pollution Control, Guangdong Provincial Key Laboratory of Soil and Groundwater Pollution Control, School of Environmental Science and Engineering, Southern University of Science and Technology, Shenzhen 518055, China

*Corresponding authors:

E-mail address: luowj@cug.edu.cn (Wenjun Luo); chenh3@sustech.edu.cn (Hong Chen)

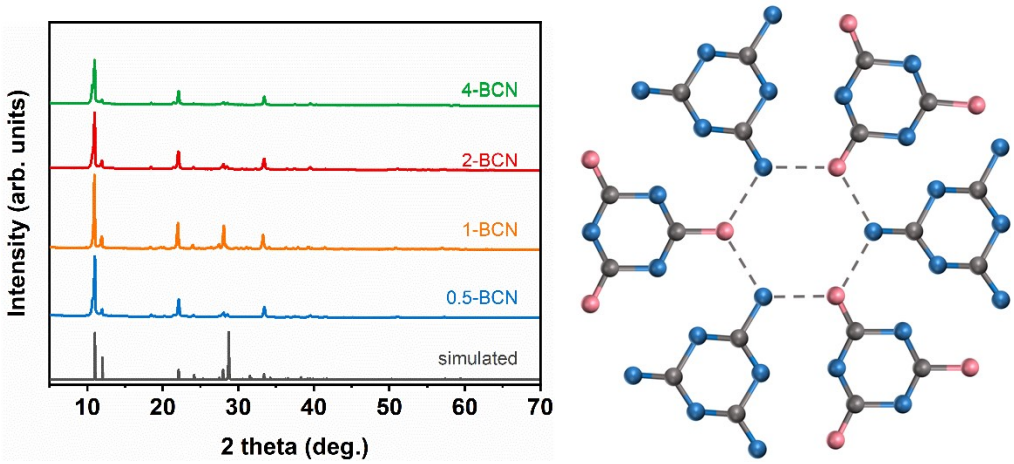

Fig. S1. XRD patterns of x-BCN (x=0.5, 1, 2, 4) with different molar ratios of HBO_3 (0.5, 1, 2, 4 mmol).

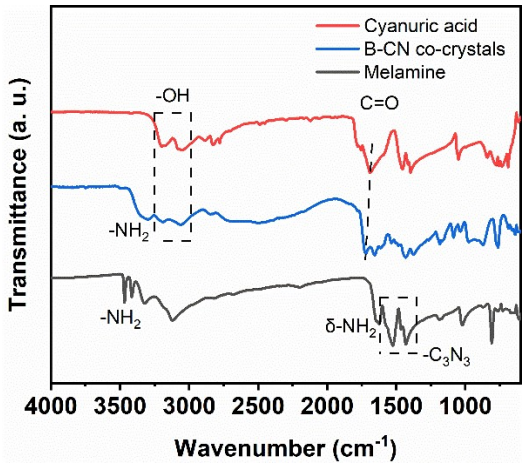

Fig. S2. The FT-IR spectra of commercial melamine, cyanuric acid and B-CN co-crystals.

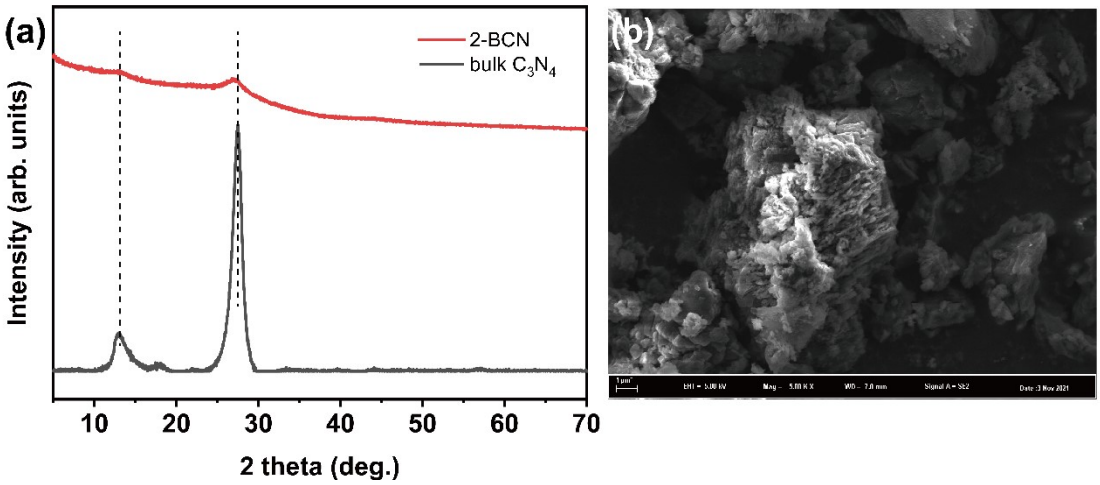

Fig. S3. The XRD pattern (a) of 2-BCN bulk C_3N_4. (b) SEM of bulk C_3N_4.

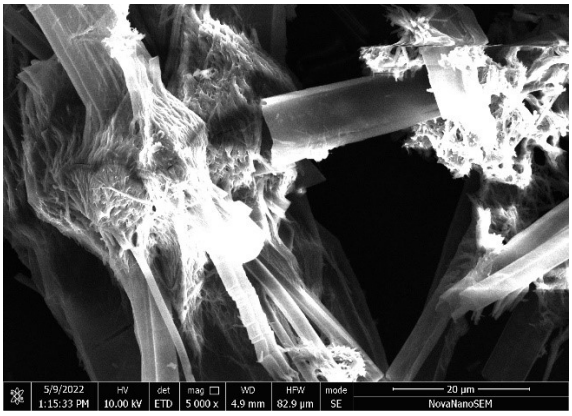

Fig. S4. SEM of carbon nitride formed without boric acid-assisted pyrolysis.

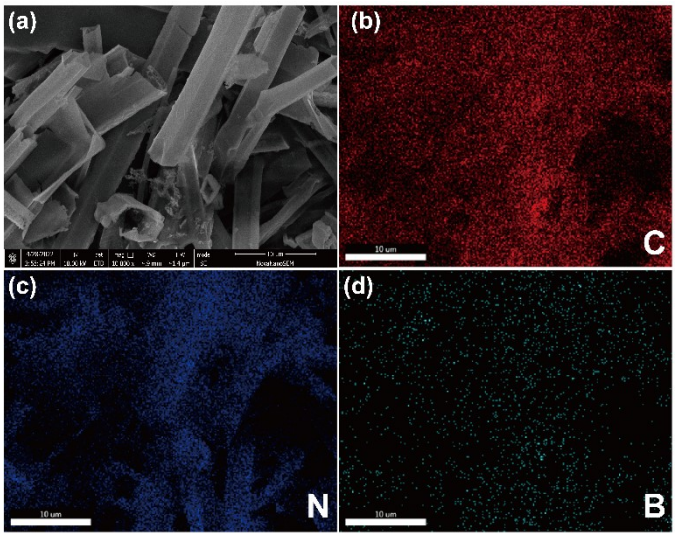

Fig. S5. SEM images of 2-BCN and correspond elements mapping of C, N, B.

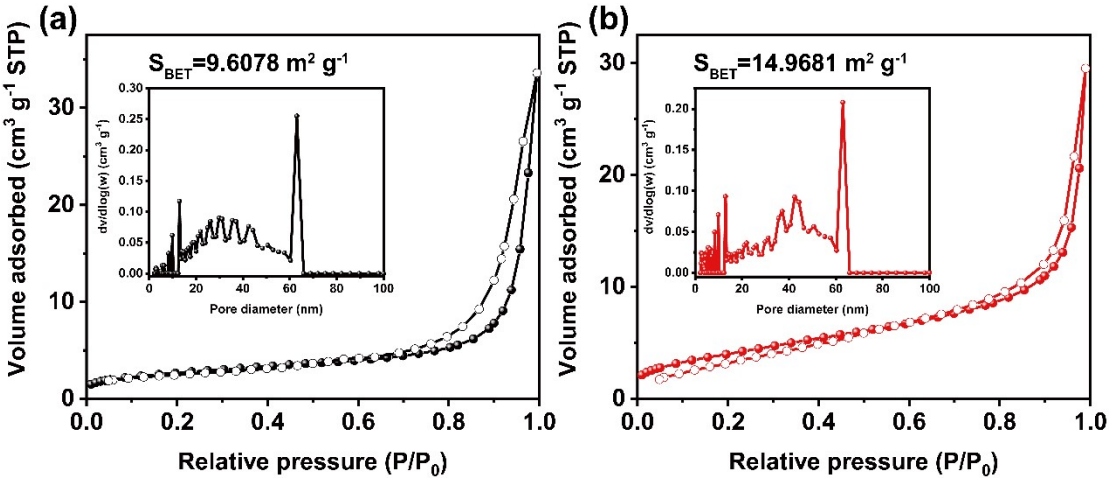

Fig. S6. N_2 adsorption-desorption isotherms and the corresponding pore size distribution curves (inset) of (a) bulk C_3N_4, (b)2-BCN.

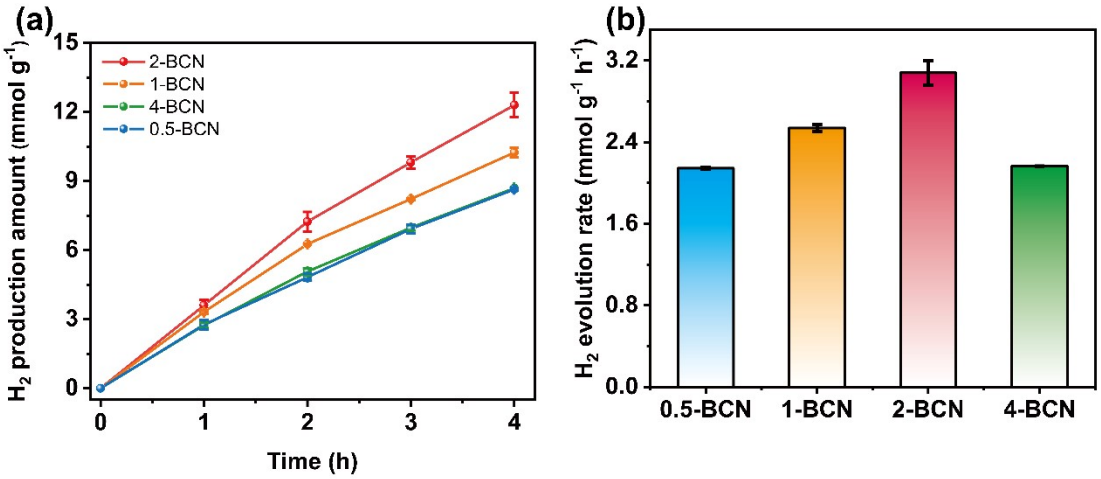

Fig. S7. (a) Photocatalytic H_2 production amount and evolution rates of x-BCN (x=0.5, 1, 2, 4).

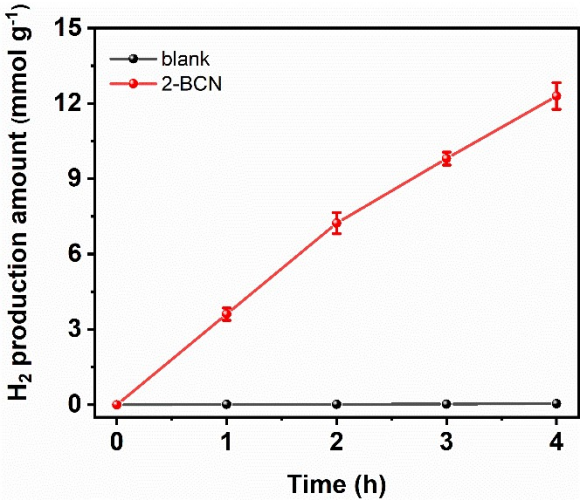

Fig. S8. Photocatalytic H_2 production amount of 2-BCN (red line) and without photocatalysts (blank line)

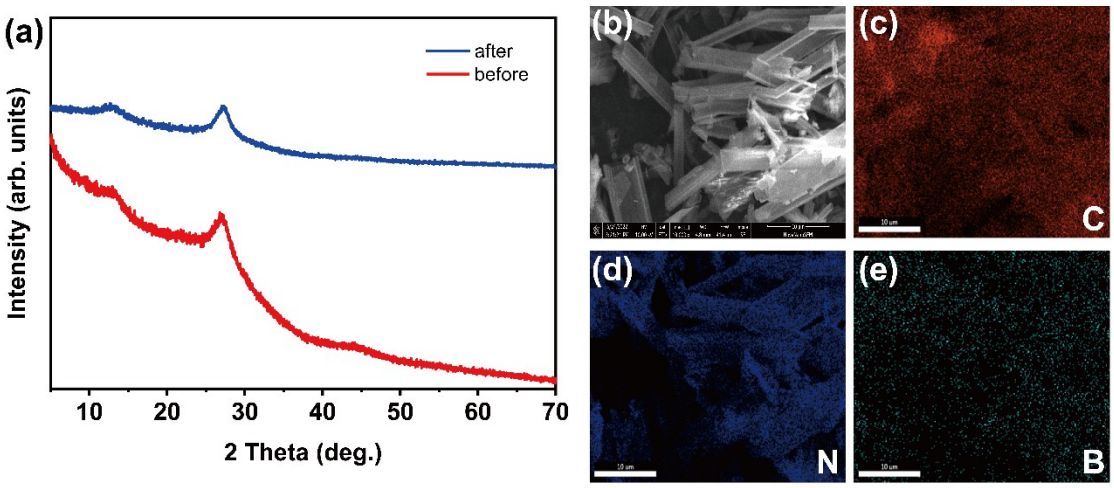

Fig. S9. (a) XRD of 2-BCN before and after eight photocatalyst hydrogen evolution. (b) SEM and (c-e) correspond elements mapping of 2-BCN after photocatalyst hydrogen evolution.

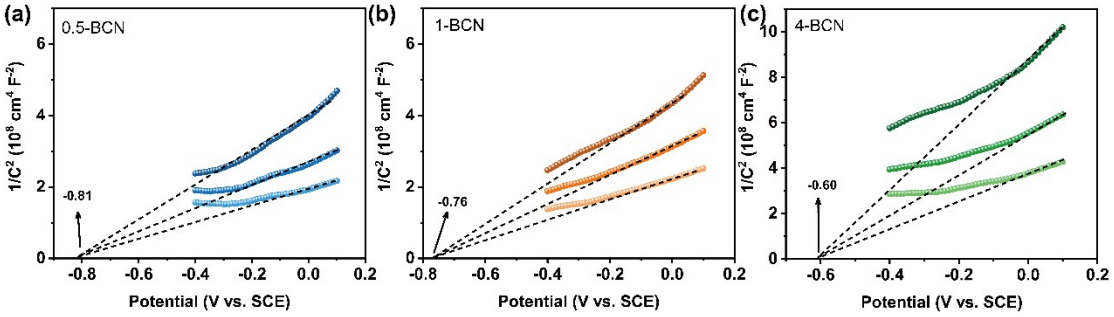

Fig. S10. (a-c) Mott-Schottky plots of x-BCN (x=0.5, 1, 4).

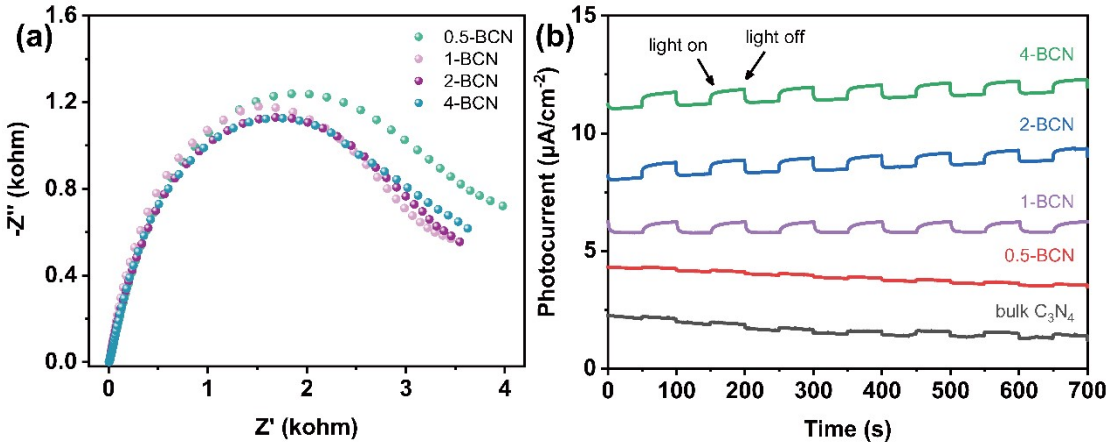

Fig. S11. (a) EIS plots and (b) transient photocurrent responses of x-BCN (x=0.5, 1, 2, 4).

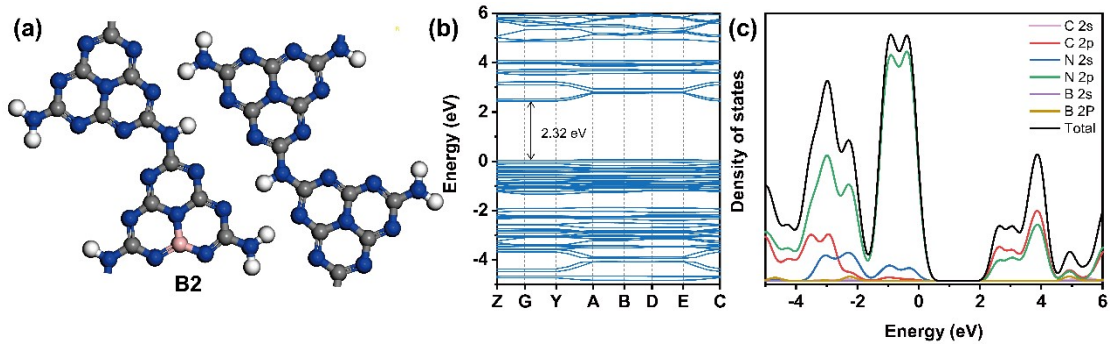

Fig. S12. (a) Structure models of x-BCN with B2-site dopants. (b) Calculated band structures and (c) corresponding density of states (DOS) calculations of x-BCN with B2-site dopants.

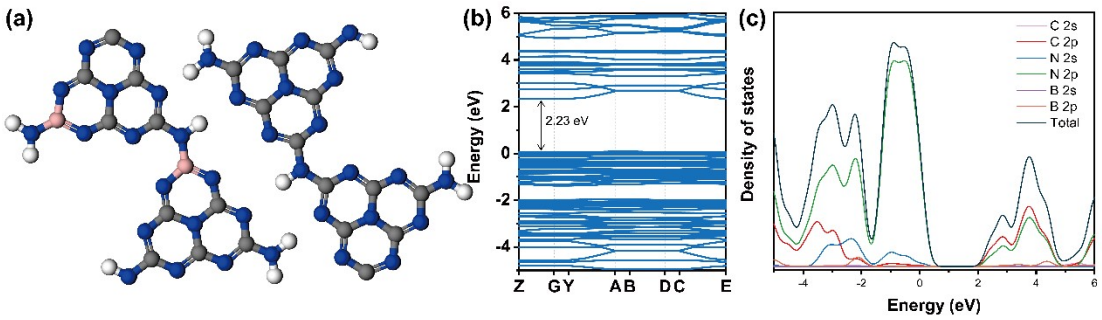

Fig. S13. (a) Structure models, (b) Calculated band structures and (c) corresponding density of states (DOS) of BCN with two C2 atoms substituted by B.

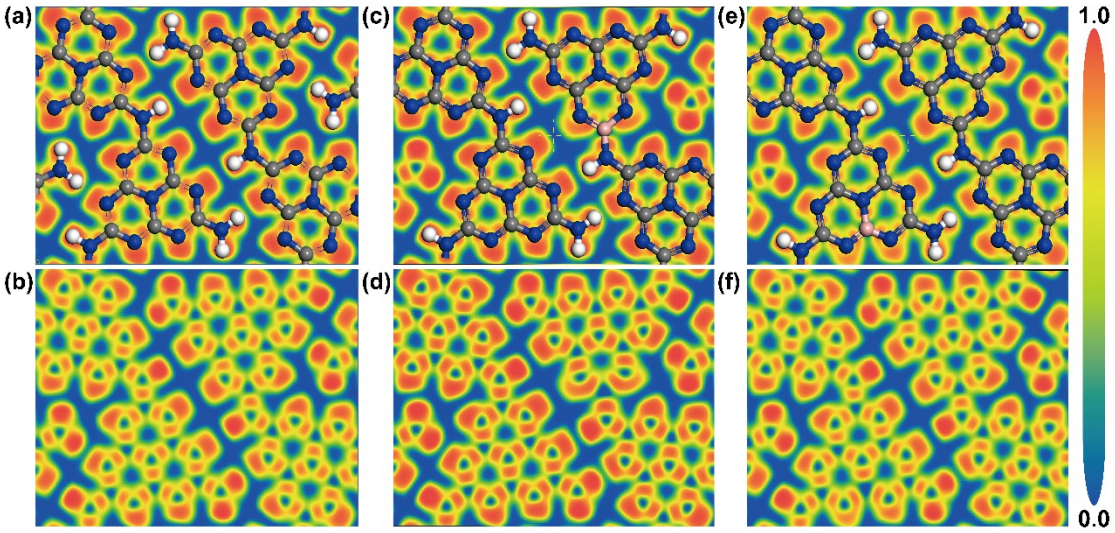

Fig. S14. Electron localization function spectrums of pristine C3N4 (a, b), x-BCN with B1-site dopants (c, d), and x-BCN with B2-site dopants (e, f).

Table S1. Comparison of photocatalytic hydrogen evolution performance over similar materials.

photocatalyst	amt. (mg)	experimental conditions	H_2 evolution rate ($\mu mol \cdot g^{-1} \cdot h^{-1}$)	Reference
P-TCN	100	80 mL H_2O and 20 mL methanol, 1 wt% Pt	67	[1]
TCN	25	25 ml H_2O and 5 mL TEOA*, 3wt% Pt	2098	[2]
UCN-200	30	45 ml H_2O and 5 mL TEOA, 3wt% Pt	1254.7	[3]
D-TCN450	25	25 ml H_2O and 5 mL TEOA, 3wt% Pt	789.2	[4]
2-BCN	**30**	45 ml H_2O and 5 mL TEOA, 3wt% Pt	**3065.8**	**This work**

*TEOA: Triethanolamine.

Table S2. Summary of the time-resolved PL decay spectra for the prepared sample bulk C_3N_4 and 2-BCN.

Sample	A_1	A_2	A_3	τ_1 (ns)	τ_2 (ns)	τ_3 (ns)	τ_{avg} (ns)	R^2
Bulk C_3N_4	162.7281	464.8410	163.6261	0.2937	1.4719	5.3829	3.5729	0.9934
2-BCN	235.0336	422.7973	143.1008	0.2972	1.2652	4.9404	3.1945	0.9929

The obtained TR-PL curves are mathematically expressed by a three-exponential equation[5]:

$$I(t) = A_1 e^{-\frac{t}{\tau_1}} + A_2 e^{-\frac{t}{\tau_2}} + A_3 e^{-\frac{t}{\tau_3}} \quad (1)$$

where, A1, A2 and A3 represent the normalized amplitudes of each decay component and τ1, τ2 and τ3 are values of the lifetime components, respectively.

$$\tau_{avg} = (A_1\tau_1^2 + A_2\tau_2^2 + A_3\tau_3^2)/(A_1\tau_1 + A_2\tau_2 + A_3\tau_3) \quad (2)$$

Reference

1. Guo S., Deng Z., Li M., et al. Phosphorus-Doped Carbon Nitride Tubes with a Layered Micro-nanostructure for Enhanced Visible-Light Photocatalytic Hydrogen Evolution[J]. Angewandte Chemie International Edition, 2016, 55(5): 1830-1834.
2. Wang W., Wang M., Li X., et al. Microwave-Assisted Catalytic Cleavage of C–C Bond in Lignin Models by Bifunctional Pt/CDC-SiC[J]. ACS Sustainable Chemistry & Engineering, 2020, 8(1): 38-43.
3. Chen L., Liang X., Wang H., et al. Ultra-thin carbon nitride nanosheets for efficient photocatalytic hydrogen evolution[J]. Chemical Engineering Journal, 2022, 442: 136115.
4. Chen L., Wang Y., Cheng S., et al. Nitrogen defects/boron dopants engineered tubular carbon nitride for efficient tetracycline hydrochloride photodegradation and hydrogen evolution[J]. Applied Catalysis B: Environmental, 2022, 303: 120932.
5. Kumar P., Vahidzadeh E., Thakur U.K., et al. C3N5: A Low Bandgap Semiconductor Containing an Azo-Linked Carbon Nitride Framework for Photocatalytic, Photovoltaic and Adsorbent Applications[J]. Journal of the American Chemical Society, 2019, 141(13): 5415-5436.